J. Membrane Biol. 129, 71–80 (1992)

The Journal of
Membrane Biology

Slow Inactivation of Tetrodotoxin-Insensitive Na^+ Channels in Neurons of Rat Dorsal Root Ganglia

Nobukuni Ogata and Hideharu Tatebayashi
Department of Pharmacology, Faculty of Medicine, Kyushu University, Fukuoka 812, Japan

Summary. Whole-cell patch-clamp experiments were performed with neurons cultured from rat dorsal root ganglia (DRG). Two types of Na^+ currents were identified on the basis of sensitivity to tetrodotoxin. One type was blocked by 0.1 nM tetrodotoxin, while the other type was insensitive to 10 μM tetrodotoxin. The peak amplitude of the tetrodotoxin-insensitive Na^+ current gradually decreased after depolarization of the membrane. The steady-state value of the peak amplitude was attained several minutes after the change of holding potential. Such a slow inactivation was not observed in tetrodotoxin-sensitive Na^+ current. The slow inactivation of the tetrodotoxin-insensitive Na^+ current was kinetically distinct from the ordinary short-time "steady-state" inactivation. The voltage dependence of the slow inactivation could be described by a sigmoidal function, and its time course had a double-exponential process. A decrease of external pH partially antagonized the slow inactivation, probably through an increased diffusion potential across the membrane. However, the slow inactivation was not due to change in surface negative charges, since a shift of the kinetic parameters along the voltage axis was not observed during the slow inactivation. Due to the slow inactivation, the inactivation curves for the tetrodotoxin-insensitive Na^+ current were shifted in the negative direction as the prepulse duration was increased. Consequently, the window current activated at potentials close to the resting membrane potential was markedly reduced. Thus, the slow inactivation may be involved in the long-term regulation of the excitability of sensory neurons.

Key Words sodium channel · tetrodotoxin · dorsal root ganglion · patch clamp · slow inactivation

Introduction

The peak amplitude of the voltage-dependent Na^+ current (I_{Na}) depends on the membrane potential. This voltage dependence was described by the steady-state Na^+ inactivation, h_∞ (Hodgkin & Huxley, 1952). The h_∞ reaches different steady-state levels within an order of milliseconds. Narahashi (1964) described the slow inactivation of I_{Na} in the lobster giant axon. The time constant of inactivation was close to 1 sec.

Adelman and Palti (1969) detected an additional type of slow inactivation in the squid giant axon. This type of inactivation had a double-sigmoidal voltage dependence, and its time constant was in the range of 30–200 sec. This mechanism, named q, was shown to be independent of the external K^+ concentration, but further properties were not measured and no explanation for this inactivation was proposed. This slow inactivation has been further investigated by Rudy (1978). Similar slow Na^+ inactivation was also reported in frog myelinated nerves (Fox, 1976; Neumcke et al., 1976).

Recently, in addition to Na^+ channels in axons of the nonmammals, the slow inactivation has been demonstrated also in Na^+ channels in rabbit cardiac Purkinje fibers (Carmeliet, 1987) and Ca^{2+} channels in frog cardiac myocytes (Kass & Scheuer, 1982; Schouten & Morad, 1989) and in rabbit portal vein (Nilius, Kitamura & Kuriyama, 1992). Thus, the slow inactivation may be general properties of voltage-gated ion channels in excitable membrane and play an important role in the regulation of ion-channel activity. However, the mechanism underlying the slow inactivation is entirely obscure, and further experimentation in this field is required to establish the precise nature of the slow inactivation. We found that one type of Na^+ channel in rat DRG exhibits a prominent slow-inactivation process. The aim of this paper is, therefore, to examine properties of the slow inactivation of Na^+ channels in mammalian neuronal membrane.

Materials and Methods

Dissociation and Culture Procedures

Procedures for dissociation and culture of the dorsal root ganglion (DRG) neurons were described previously (Tatebayashi & Ogata, 1992). Rats were killed by decapitation under ethylether anesthe-

sia. The preparations were obtained from newborn (1–2 days postnatal) rats. The DRG were dissected out and incubated at 36°C for 30–40 min in Ca^{2+}- and Mg^{2+}-free saline, containing 0.25% trypsin (Type XI, Sigma). The ganglia were then mechanically dissociated with a fire-polished Pasteur pipette. Dissociated cells were kept in Krebs solution at room temperature. The cells were plated on glass coverslips coated with poly-L-lysine (Sigma) and maintained in a humidified incubator containing 5% CO_2 in air at 35°C in Dulbecco's modified Eagle medium supplemented with 10% fetal bovine serum (GIBCO), penicillin (40 IU/ml), and streptomycin (40 ng/ml). After one to two days in culture, cytosine β-D-arabinofuranoside (Sigma) was added to cultures to suppress the growth of nonneuronal cells. Subsequent medium changes were done at three- to four-day intervals. Cells between three to four weeks in culture were used.

Electrical Recording

The methods for electrical recording used in the present study were similar to those previously described (Ogata, Yoshii & Narahashi, 1990). Membrane currents were recorded with the whole-cell patch-clamp technique (Hamill et al., 1981). The DC resistance of suction electrodes was 0.5–0.8 MΩ. The pipette solution contained (in mM): 135 CsF, 10 NaF, and 5 HEPES. The pH of the pipette solution was adjusted to 7.0 with CsOH. The external solution contained (in mM): 100 NaCl, 5 CsCl, 1.8 $CaCl_2$, 1 $MgCl_2$, 5 HEPES, 20 tetraethylammonium-Cl, and 25 glucose. The pH of the external solution was adjusted to 7.4 with NaOH.

All the experiments were performed with an on-line system which has been developed by M. Yoshii and N. Ogata, using a personal computer (PC-286V, EPSON, Tokyo, Japan). Membrane currents passing through the pipette were recorded by a current-to-voltage converter designed by M. Yoshii (Narahashi, Tsunoo & Yoshii, 1987) and stored on hard disk. Compensation for the series resistance was performed by adding a part of the output voltage of the current recording to the command pulse. Capacitive and leakage currents were subtracted digitally by the P-P/4 procedure (Ogata et al., 1990). The liquid junction potential between internal and external solutions was compensated for by adjusting the zero-current potential to the liquid junction potential. Only cells showing an adequate voltage and space clamp (Ogata & Tatebayashi, 1990) were used. The baseline of current at holding potential was continuously recorded with an ink writer. Experiments were started after an initial stabilization period of about 15 min. Programmed sequences of voltage pulses were applied to the preparation from the computer using a digital-to-analog converter.

Experiments were performed at room temperature (21–23°C). Results are expressed as means ± SEM, and n represents the number of cells. Exponential fits were determined by computer using a nonlinear sum of the least-squares fitting routine.

Results

Neurons in rat DRG could be divided into three groups depending on their responsiveness to tetrodotoxin (TTX) (Kostyuk, Veselovsky & Tsyndrenko, 1981; Ogata & Tatebayashi, 1992*a,b,c*). The first group was characterized by I_{Na} which was totally suppressed by a low concentration of TTX (Fig. 1A_1). The second group had I_{Na} which is insensitive to TTX (Fig. 1A_2). The third group of neurons had both types of I_{Na} (*not shown*). As has been reported (Ogata & Tatebayashi, 1992*a*), the TTX-insensitive I_{Na} is distinct from Ca^{2+} channel currents. The TTX-sensitive and TTX-insensitive I_{Na} have different voltage dependence for activation (Fig. 1*B* and *C*). The activation levels were about −60 mV for the TTX-sensitive I_{Na} and about −40 mV for the TTX-insensitive current. Peak amplitudes were obtained at −30 and −10 mV, respectively, for the TTX-sensitive and TTX-insensitive I_{Na}. Detailed kinetic properties of the two types of I_{Na} in rat DRG have been described elsewhere (Ogata & Tatebayashi, 1992*b*).

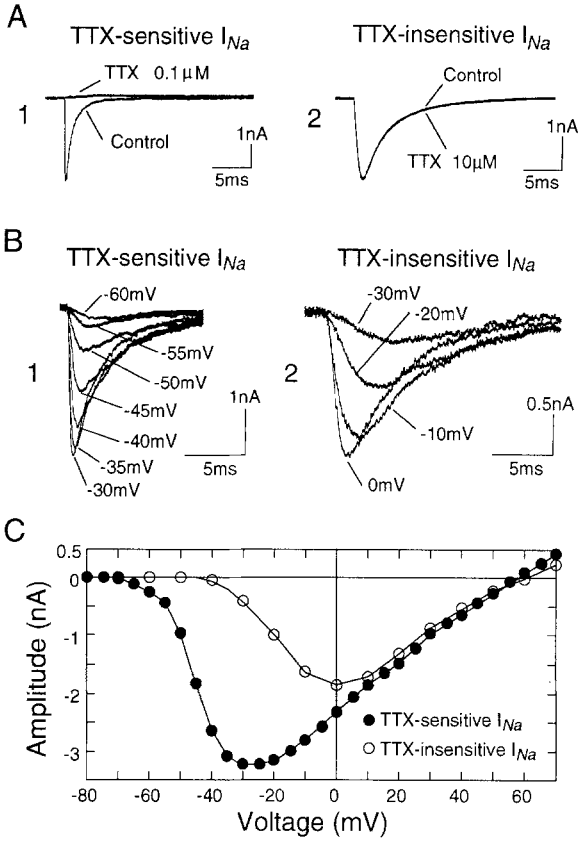

Fig. 1. Typical examples of the two types of Na^+ channels in neurons of the rat dorsal root ganglia (DRG). (*A*) Na^+ currents (I_{Na}) in the control solution and in the presence of 0.1 μM (*1*) or 10 μM (*2*) tetrodotoxin (TTX) were superimposed. (*B*) A family of I_{Na} were evoked by 30-msec voltage steps to indicated potentials from a holding potential (V_h) of −80 mV. B_1 was recorded from the cell whose I_{Na} was totally blocked by 1 μM TTX. B_2 was recorded in the presence of 1 μM TTX. (*C*) Current-voltage curves obtained from cells shown in *B*. Peak amplitude of I_{Na} was plotted against test potential. In this and subsequent figures, downward and upward deflections represent inward and outward currents, respectively.

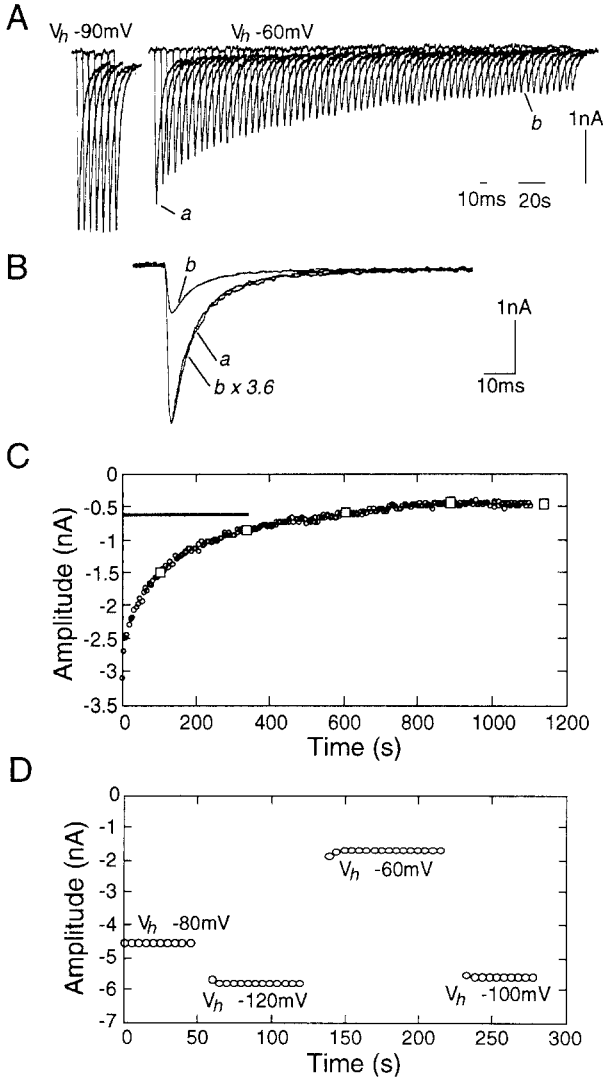

Fig. 2. Slow inactivation of TTX-insensitive I_{Na} in rat DRG. (*A*) I_{Na} was evoked by voltage step to −10 mV from a V_h of −90 mV (left traces) and −60 mV (right traces). Between two groups with different V_h, 10 sec was interposed. (*B*) Current traces labeled *a* and *b* in *A* are shown superimposed in an expanded time scale. The amplitude of trace *b* was scaled 3.6-fold to match the peak current of trace *a*. (*C*) The peak amplitude of I_{Na} in *A* was plotted against time. V_h was changed to −60 from −90 mV 10 sec before time 0. The bar indicates the period during which the traces in *A* were recorded. Open squares indicate the amplitude of I_{Na} evoked at intervals longer than 200 sec. (*D*) TTX-sensitive I_{Na} was activated intermittently as in *A* and plotted against time. *A–C* were recorded in the presence of 1 μM TTX. *D* was recorded in the absence of TTX from the cell whose I_{Na} was totally blocked by 1 μM TTX.

Slow Inactivation of TTX-insensitive I_{Na}

Peak amplitude of I_{Na} evoked by a voltage step to −10 mV became progressively smaller after the transition of V_h from −90 to −60 mV in all of the 56 TTX-insensitive cells examined (Fig. 2*A*). The long periods of time (on the order of minutes) were necessary for a transition from one steady-state level to another following a change in V_h. This slowly developing inactivation at the depolarized V_h is distinct from the fast inactivation which reaches different steady-state levels within an order of milliseconds. The activation and inactivation time courses of I_{Na} were not affected during the slow inactivation (*see* the superimposed traces in Fig. 2*B*).

The steady-state value of the peak amplitude of I_{Na} was obtained about 800 sec after the shift of V_h (Fig. 2*C*). Since the peak amplitude of I_{Na} evoked at intervals of 300 sec (open squares in Fig. 2*C*) was similarly affected by the V_h shift, the reduction of the peak amplitude was not due to the use-dependent effect of the repetitive I_{Na} activation. In contrast to the marked slow inactivation in the TTX-insensitive I_{Na}, the typical slow inactivation was not observed in any of the 10 TTX-sensitive I_{Na} examined. Although three of the TTX-sensitive I_{Na} showed a slowly developing decrease of the peak amplitude after transition of V_h, the decrease was irreversible in all three cases. Thus, only the TTX-insensitive cells were used for subsequent experiments.

Figure 3 compares the ordinary fast inactivation ($h_{0.5s}$) with the slow inactivation. The duration of 0.5 sec is generally thought to be sufficient for neuronal Na^+ channels to attain steady-state inactivation (Ogata et al., 1990; Ogata & Tatebayashi, 1990). The $h_{0.5s}$ was retained constant before, during and after the shifts of V_h, indicating that the ordinary short-period inactivation kinetics in the sense of Hodgkin and Huxley (1952) is retained in channels which escaped the slow inactivation. The slow inactivation was bidirectional, i.e., the identical time courses of the change in the peak amplitude of I_{Na} were observed in both cases of V_h shifts from −90 to −60 mV and from −60 to −90 mV.

Time Course of Slow Inactivation

Three sets of overlapped current traces in Fig. 4*A* illustrate the successive I_{Na} after transitions of V_h from an initial value of −90 to −60, −50 and −40 mV. The time course of slow inactivation became faster as the V_h level was set to a more depolarized level. To facilitate the comparison, peak amplitudes of I_{Na} were normalized in Fig. 4*B*. The time course of the slow inactivation was best described with a double-exponential function in all the V_h examined (Fig. 4*C*). Both the fast and slow time constants (τ_f and τ_s) became progressively shorter when the V_h was set to a more positive level, whereas the ratio of the amplitudes of the two time constants (A_f and A_s) was relatively constant. Time constants and their

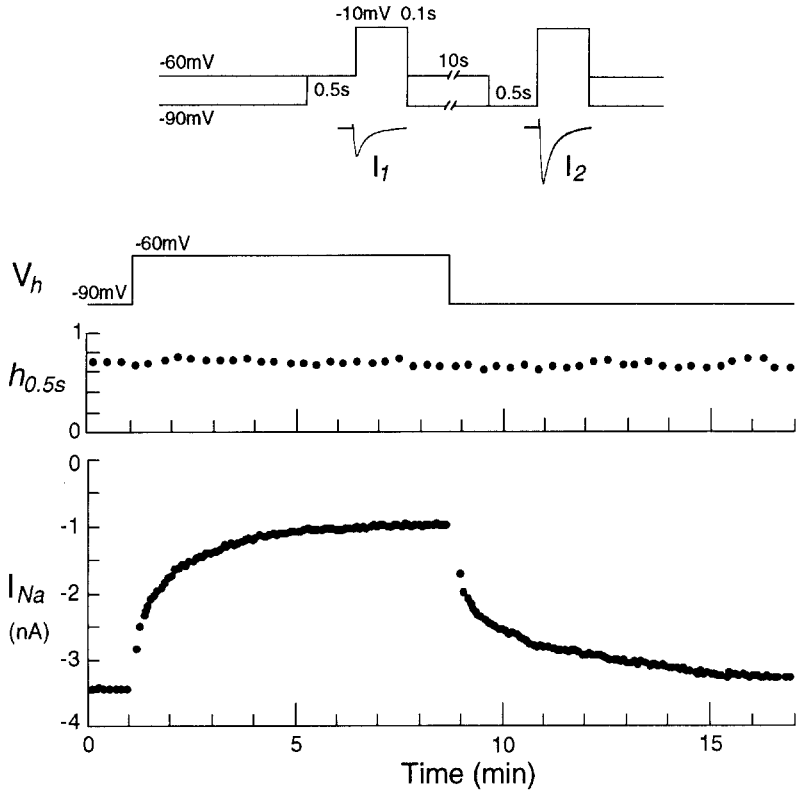

Fig. 3. Time course of $h_{0.5s}$ and slow inactivation of TTX-insensitive I_{Na}. The value $h_{0.5s}$ was measured from I_1/I_2 where I_1 and I_2 were peak amplitudes of currents evoked by test pulses to -10 mV applied from prepulse levels of -60 mV (I_1) and -90 mV (I_2), respectively. When V_h was set to -90 mV, the first test pulse was preceded by a 0.5-sec depolarizing prepulse to -60 mV. Likewise, when V_h was set to -60 mV, the second test pulse was preceded by a 0.5-sec hyperpolarizing prepulse to -90 mV (*see* inset diagram). I_{Na} was evoked by a step depolarization to -10 mV for 100 msec delivered every 5 sec. V_h was at first -90 mV and shifted to -60 mV, and returned to -90 mV. V_h, $h_{0.5s}$ and peak amplitude of I_{Na} were plotted against time, respectively. In this and in all subsequent figures, current traces were recorded in the presence of 1 μM TTX (i.e., I_{Na} were all TTX insensitive).

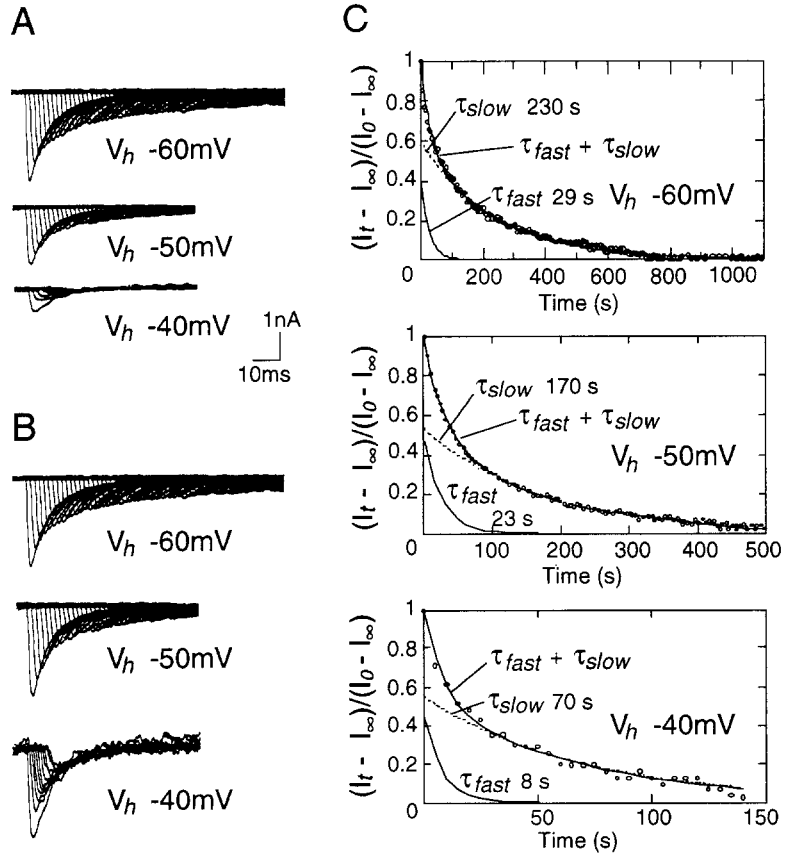

Fig. 4. Double-exponential fits to the time course of slow inactivation. (*A*) Subsequent to a 10-sec pause after the switching of V_h from -90 mV to potential levels of -60, -50 or -40 mV, I_{Na} was intermittently evoked by voltage step to -10 mV delivered every 5 sec. Successive current traces are shown overlapped at regular intervals. (*B*) Initial peak amplitudes of traces in *A* were normalized to facilitate the comparison. (*C*) The value, $(I_t - I_\infty)/(I_0 - I_\infty)$, was plotted as a function of time. I_0 and I_t are peak amplitudes of I_{Na} at time 0 and t, respectively. I_∞ is the steady-state level of I_{Na} at the new V_h.

Table. The time course of the peak sodium current after a step change of the holding potential (V_h) as evaluated by fitting the following Equation to the experimental points: $I_{(t)} = A_f \cdot \exp(-t/\tau_f) + A_s \cdot \exp(-t/\tau_s)$

Step change of V_h (mV)	A_f	A_s	τ_f (sec)	τ_s (sec)
−90 to −60	0.42 ± 0.03	0.58 ± 0.03	26.5 ± 3.6	217.0 ± 28.4
−60 to −90	0.43 ± 0.04	0.57 ± 0.04	21.3 ± 2.8	207.5 ± 15.9
−90 to −50	0.41 ± 0.02	0.59 ± 0.02	17.3 ± 2.1	162.5 ± 13.7
−90 to −40	0.43 ± 0.03	0.57 ± 0.03	8.3 ± 0.6	80.5 ± 5.9

Results are expressed as mean ±SEM (n = 4).

amplitudes obtained at different V_h are summarized in the Table.

Effects of pH on the Slow Inactivation

A long-term change in V_h could produce changes in the negative charge density of the internal surface of the membrane by a phospholipid flip-flop mechanism (McNammee & McConnell, 1973; McLaughlin & Harari, 1974). The parameters which control the Na^+ channel gating mechanism are affected by changes in external surface charges (Chandler, Hodgkin & Meves, 1965). Thus, it is conceivable that the slow inactivation is due to the parallel shift of the voltage axis of the steady-state inactivation, thus decreasing the availability of Na^+ channels. To examine this possibility, the pH of the external solution was changed during transitions of V_h.

As shown in Fig. 5*A*, a change of pH from 7.3 to 5.3 caused a parallel shift of the current-voltage curves for the TTX-insensitive I_{Na} in the depolarizing direction by 10 mV. Thus, the test potential to +10 mV produced I_{Na} of similar peak amplitudes in the two solutions with different pH. Although H^+-activated current has been reported in rat DRG (Krishtal & Pidoplichko, 1980), this current did not affect the measurement due to its instantaneous and transient nature. The slow inactivations induced by transitions of V_h to −60 and to −45 mV were partially antagonized by a change of pH from 7.3 to 5.3 (Fig. 5*B*). The same results were obtained in all of the five cells tested.

The slow inactivation thus could be due to a change in membrane surface charges. However, this possibility was excluded by the observation that a shift of the kinetic parameters of Na^+-channel activation along the voltage axis was not observed during the slow inactivation (compare curve *a* with *c* in Fig. 5*A*). The possibility of current-dependent inactivation due to build-up of free intracellular Na^+ ions in the immediate vicinity of the channel can also be ruled out by the above experiment, since the reversal potentials for the two current-voltage curves were not affected by the slow inactivation.

Recovery from Inactivation

To examine further whether the slow inactivation is merely an extension of the ordinary fast voltage-dependent inactivation or it represents the inactivation process which is totally distinct from it, the recovery process from inactivation was studied. Figure 6*A* shows an experimental protocol and a typical example of the recovery process from inactivation. As shown in Fig. 6*B*, upper panel, the inactivation induced by the prepulse (V_{pre}) recovered exponentially during recovery periods (ΔT) at various potential levels (ΔV). It should be noted that the recovery from inactivation with ΔV of −40 or −35 mV was again decreased after it attained its peak value at ΔT of 160 msec. Such a reduction was observed also with ΔV of −50, −55 and −60 mV when examined with longer ΔT (Fig. 6*B*, lower panel). These potentials correspond to the potential levels which cause the slow inactivation.

Conditioning pulses (V_{pre}) to various potential levels (ΔV) were followed by a test pulse (V_{test}) at varying intervals (ΔT) (*see* inset diagram of Fig. 7*A*). The amplitude of I_{Na} evoked by V_{test} (I_{test}) was much the same with various conditioning pulses ranging from −60 to +70 mV at ΔT longer than 10 sec. Namely, the large membrane depolarization does not affect the overall time course of the slow inactivation. The different time courses with ΔT less than 5 sec were probably due to the different time courses of the ordinary voltage-dependent inactivation process, because the currents did not fully recover from inactivation when the recovery voltage was set to −80 mV, where no slow inactivation occurs. These results might suggest that the slow inactivation does not proceed directly from open or fast inactivated

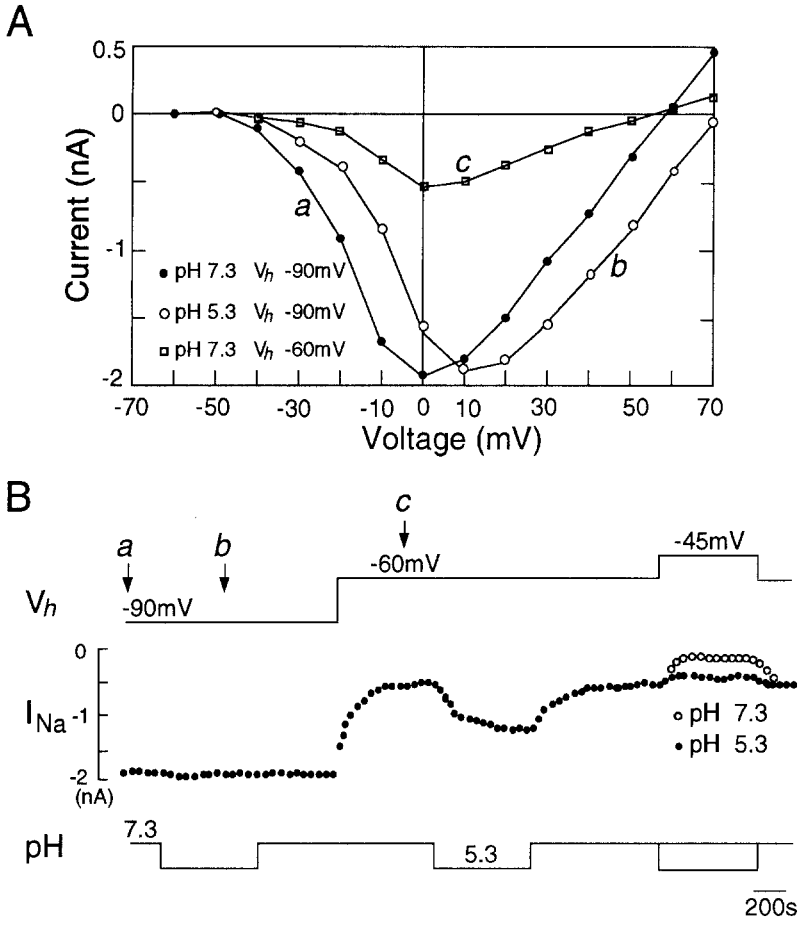

Fig. 5. The effect of external pH on the slow inactivation of the TTX-insensitive I_{Na}. (*A*) Effects of changes in external pH (from 7.3 to 5.3) and V_h (from −90 to −60 mV) on the current-voltage relationship. A family of currents were evoked by a 30-msec step to various potentials (−70 to +70 mV) from V_h of −90 mV (curves *a* and *b*) or −60 mV (curve *c*). Peak amplitude of I_{Na} was plotted against the value of test potential. Filled circles (curve *a*) and open squares (curve *c*), pH 7.3; open circles (curve *b*), pH 5.3. The pH of the external solution was lowered by adding HCl. (*B*) The TTX-insensitive I_{Na} was intermittently evoked by a 30-msec step to 10 mV delivered every 20 sec during changes in V_h and external pH, and its peak amplitude was plotted as a function of time.

channels and the ordinary fast voltage-dependent inactivation can recover independently of the slow inactivation.

Time and Voltage Dependence of Slow Inactivation

The steady-state inactivation curve for the TTX-insensitive Na^+ channels obtained with relatively short prepulses does not represent the true steady-state inactivation of the channel due to the presence of slow inactivation. Thus, we measured the steady-state inactivation using various prepulse durations maximally extended to 5 min. Figure 8*A* shows the typical example of the steady-state inactivation measured with 0.5-sec prepulse ($h_{0.5s}$). In order to minimize the error arising from a possible fluctuation of I_{Na}, the control I_{Na} was measured 10 sec prior to each V_{test}. The 10-sec interval was sufficient to recover from the inactivation due to $V_{control}$. Experiments in which the amplitude of $V_{control}$ changed more than 5% were discarded.

A plot of the normalized I_{Na} ($I_{test}/I_{control}$) against V_{pre} gives a measure of the voltage dependence of inactivation at time ΔT ($h_{\Delta T}$) (Fig. 8*B*). The $V_{1/2}$, the conditioning potential level where I_{Na} is one-half maximal, was progressively shifted in the negative direction when ΔT was increased from 50 to 500 msec, 1 sec, 30 sec and 5 min. The slope factor was also increased. All the $h_{\Delta T}$ curves, including the curve for ΔT of 5 min, could be described by Boltzmann's equation (*see* legend). The $h_{\Delta T}$ curves were shown superimposed in Fig. 8*C*. Similar observations were reproducible in all of the five TTX-insensitive I_{Na}. $V_{1/2}$ and the slope factor were -40.1 ± 0.8 mV and 4.6 ± 0.3 mV ($n = 4$) with ΔT of 0.5 sec and -65.2 ± 1.2 mV and 6.5 ± 0.4 mV ($n = 4$) with ΔT of 5 min, respectively. An additional intriguing point was that the $I_{test}/I_{control}$ value was rather decreased at hyperpolarized potential levels in all the steady-state inactivation curves except for the curve for ΔT of 5 min (Fig. $8B_5$). This decrease was more prominent when ΔT was shorter.

Discussion

The results presented here show that there is a very slow component of the inactivation of Na^+ channels in neurons of the rat DRG. This slow inactivation

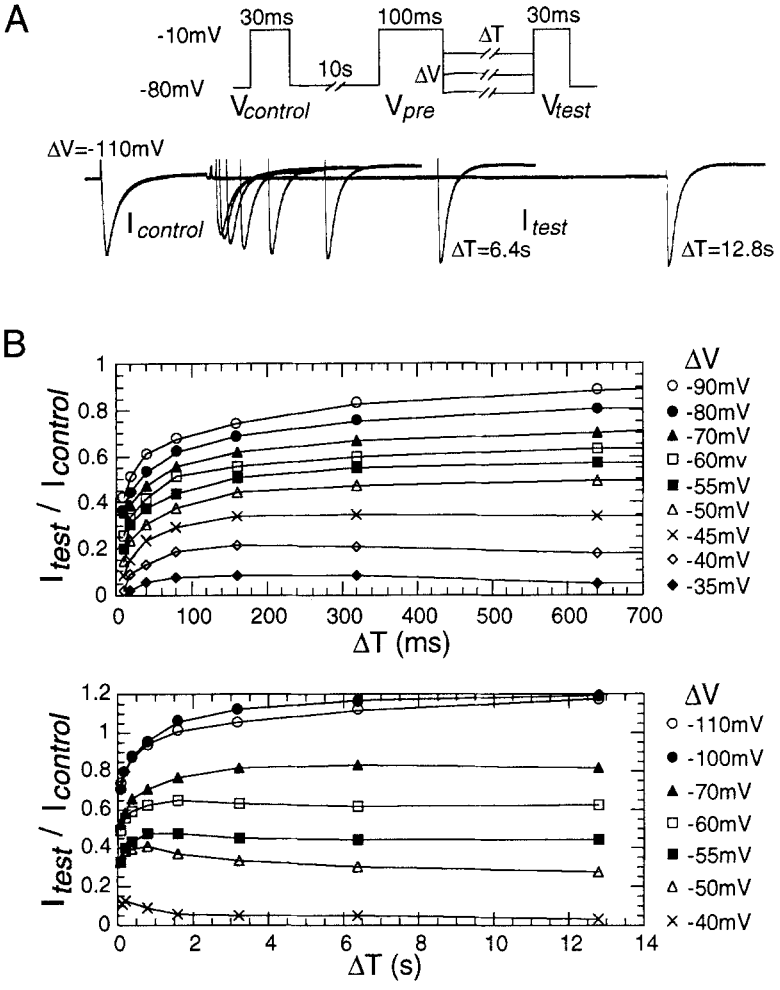

Fig. 6. Recovery from inactivation of the TTX-insensitive I_{Na} examined under different recovery voltages. (*A*) Experimental protocol and a typical example of current traces. Two identical step depolarizations to −10 mV for 30 msec were applied 10 sec prior to ($V_{control}$) and ΔT msec or sec after (V_{test}) the conditioning prepulse (V_{pre}). V_{pre} was stepped to −10 mV for 100 msec. The duration (ΔT) and the voltage (ΔV) of the recovery period were changed to various values. The currents in response to $V_{control}$ ($I_{control}$) and currents in response to V_{test} (I_{test}) were shown superimposed. ΔT was increased from 100 msec to 12.8 sec. (*B*) $I_{test}/I_{control}$ was plotted as a function of ΔT.

was induced by changes in V_h in fully reversible and voltage-dependent manners. The slow inactivation had kinetics several orders of magnitude slower than the kinetics of the ordinary short-term inactivation (in the millisecond range) described by Hodgkin and Huxley (1952). Since, in rat DRG neurons where two types of Na^+ channels coexist, only the TTX-insensitive Na^+ channel revealed the slow inactivation; the slow inactivation appears to be a physiological property of the membrane rather than some experimental artifact.

Slow inactivation of the Na^+ channels has originally been demonstrated in squid axons (Adelman & Palti, 1969; Chandler & Meves, 1970; Rudy, 1978). These slow inactivations took a hundred milliseconds to seconds to develop. The slow inactivation observed in this study had a time course on the order of minutes. Such an extremely slow inactivation process has been reported in frog myelinated fibers as "ultra-slow inactivation" (Fox, 1976) and also in rabbit cardiac Purkinje fibers (Carmeliet, 1987). The slow inactivation has also been observed in Ca^{2+} channels from *Aplysia* neurons (Adams & Gage, 1979), frog ventricular myocytes (Schouten & Morad, 1989), calf or dog Purkinje fiber (Kass & Scheuer, 1982) and rabbit portal vein (Nilius et al., 1992).

Since the slow inactivation developed independently of the ordinary fast inactivation (Figs. 6 and 7), it is suggested that the slow inactivation is a process distinct from the fast inactivation and they might be kinetically unlinked. This is consistent with the observation by Rudy (1978) that although internal perfusion with pronase blocked the fast inactivation of Na^+ channels, the slow inactivation remained. Since our experiments were performed under the condition in which both external and internal K^+ were replaced with Cs^+, the possible involvement of external K^+ concentration in the slowing of the Na^+-channel inactivation (Narahashi, 1964; Adelman & Palti, 1969) can be ruled out.

Since $[Ca^{2+}]_i$ regulates voltage-gated Ca^{2+} chan-

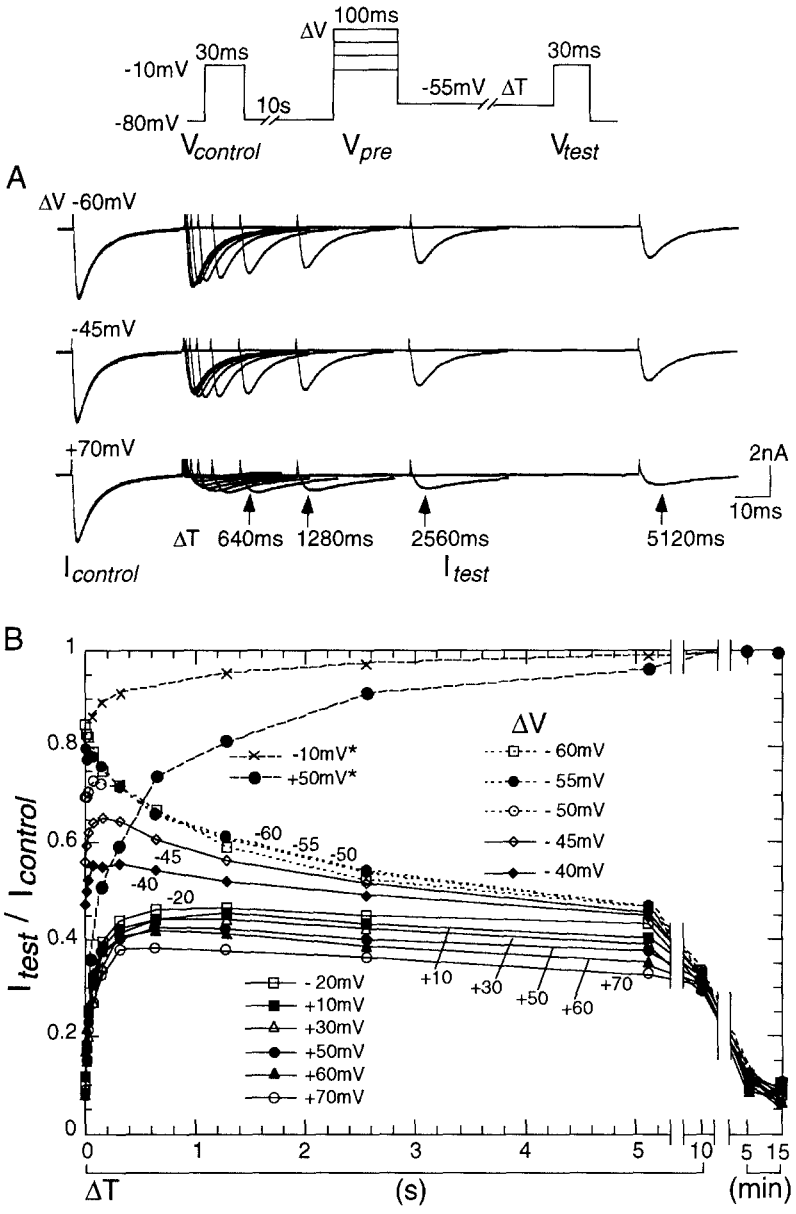

Fig. 7. Recovery from inactivation of the TTX-insensitive I_{Na} examined under different conditioning voltages and depolarized (−55-mV) recovery periods. Inset illustrates experimental protocol. Two identical step depolarizations to −10 mV for 30 msec were applied 10 sec prior to ($V_{control}$) and ΔT sec after (V_{test}) the conditioning prepulse (V_{pre}). The duration of V_{pre} was 100 msec. The voltage of V_{pre} (ΔV) was changed to various values. ΔT was increased from 10 msec to 15 min. (*A*) Typical examples of currents in response to $V_{control}$ ($I_{control}$) or to V_{test} (I_{test}) were shown superimposed. (*B*) $I_{test}/I_{control}$ was plotted as a function of ΔT. Recovery time courses for the recovery potential of −80 mV were also shown (ΔV of −10 and +50 mV labeled with asterisk).

nels (Brehm & Eckert, 1978) or even the receptor-operated ion channels (Chen et al., 1990), it is possible that the slow inactivation is mediated by a change in $[Ca^{2+}]_i$. However, Schouten and Morad (1989) suggested that a $[Ca^{2+}]_i$-independent process is responsible for the slow inactivation of I_{Ca}, since interventions which reduce or increase the level of intracellular Ca^{2+} had no significant effect on the kinetics of the slow inactivation. Similarly, the slow inactivation of I_{Na} in squid axons was not Ca^{2+}-dependent (Rudy, 1978).

The time course of the slow inactivation of TTX-insensitive I_{Na} in rat DRG could be described by a double-exponential function with two time constants in the range of seconds and minutes, respectively (Fig. 4). Such second-order kinetics of the slow inactivation has been shown in Na^+ channels of frog myelinated nerve (Fox, 1976) and in Ca^{2+} channels of rabbit portal vein (Nilius et al., 1992). The voltage dependence of the slow inactivation was fitted by the following sigmoidal function of V_h

$$h_\infty = 1/[1 + \exp\{(V_h - V_{1/2})/\kappa]$$

with a slope factor of $\kappa = 6.1$ mV and a midpoint potential of $V_{1/2} = -64$ mV (Fig. $8B_5$). Such a sigmoidal dependence of the Na^+ channel availability on V_h suggests that the distribution of charged components (dipoles or particulated complexes) within the membrane may be altered by changes of the

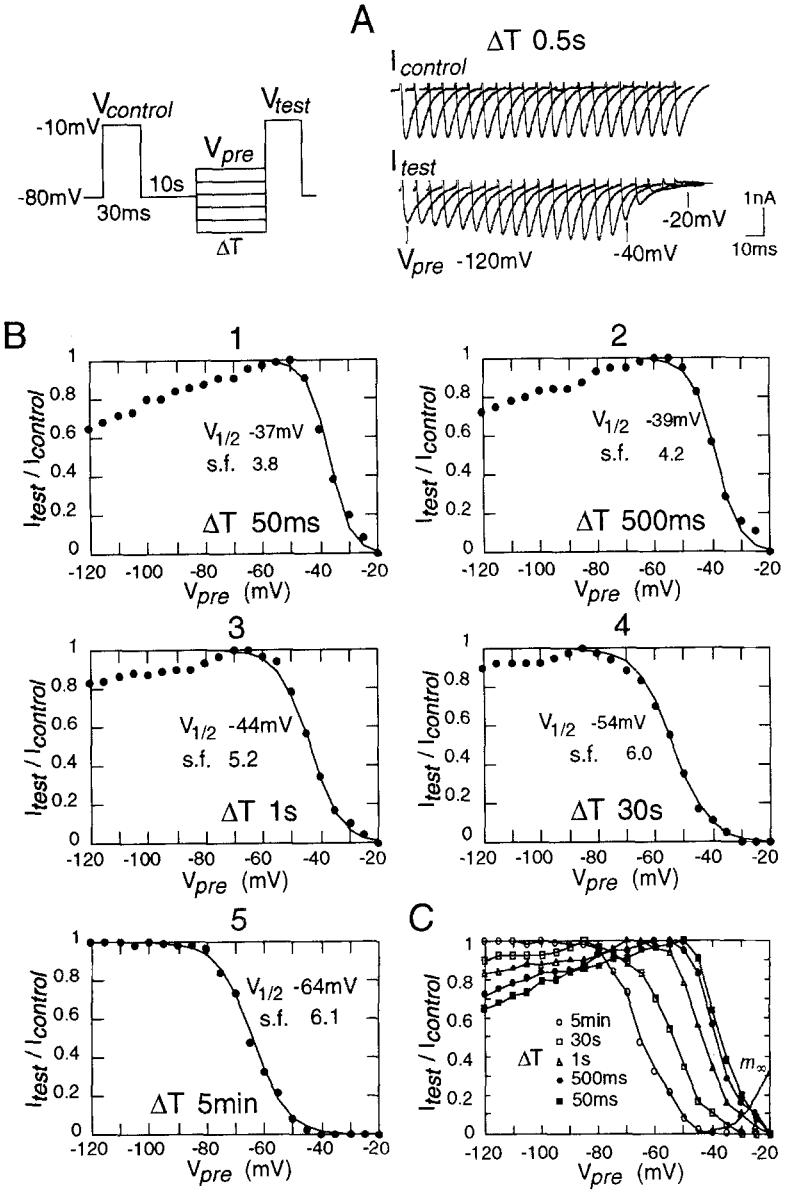

Fig. 8. The inactivation curves measured with different prepulse durations in the TTX-insensitive I_{Na}. Inset illustrates experimental protocol. Two identical step depolarizations to −10 mV for 30 msec were applied 10 sec prior ($V_{control}$) and immediately subsequent (V_{test}) to the conditioning prepulse (V_{pre}) from V_h of −80 mV. The potential level of V_{pre} was changed from −120 to −20 mV in 5-mV steps. Duration of V_{pre} (ΔT) was changed from 50 msec to 5 min. (*A*) Currents evoked by $V_{control}$ ($I_{control}$) and currents evoked by V_{test} (I_{test}) are shown overlapped at regular intervals. ΔT was 0.5 sec. (*B*) The peak amplitude of I_{test} was divided by the peak amplitude of the matched $I_{control}$ and plotted as a function of V_{pre}. The smooth curves were drawn according to the following Equation (*see* Table):

$$I_{test}/I_{control} = 1/(1 + \exp[(V_{pre} - V_{1/2})/\kappa])$$

where $V_{1/2}$ is the V_{pre} where I_{Na} is one-half maximal, and κ is the slope factor. Inactivation curves in *B* were shown superimposed in *C*.

electric field strength, assuming that the displacement of charges directly controls the long-term steady-state channel availability. The charged components are equally distributed between the conducting and the blocking configurations at $V_{1/2}$. Neumeke et al. (1976) have proposed an electrodiffusion model in which charged components diffuse slowly within the membrane. Their transverse distribution controls the availability of sodium channels at a given potential.

The slow inactivation characteristic of the TTX-insensitive Na^+ channels appears to play an important role in the regulation of cellular long-term excitability. The inactivation curve obtained under steady-state conditions (5-min prepulse) showed a shift by approximately 20 mV towards negative potentials in comparison with the curve obtained using 1-sec prepulses. This shift greatly reduced the overlap between the activation (m_∞) and inactivation curves (*see* Fig. 8*C*). These results indicate that after approximately 5 min, no stationary inward current (window current) at membrane potentials between −40 and −20 mV can be expected. Such a window current which is activated at potentials close to the resting membrane potential could obviously have an important role in modulating repetitive firing, acting as a 'pacemaker' current which drives the membrane potential back towards threshold after an action potential (Hotson, Prince & Schwartzkroin, 1979). Thus, a reduction of the window current would cause a profound change in cellular excitability.

Since two types of Na^+ channels in rat DRG

have different voltage- and time-dependent inactivation characteristics (Kostyuk et al., 1981; Ogata & Tatebayashi, 1992*b*), the number of functional Na^+ channels could be modulated depending on the channel type and the membrane potential. The availability of the TTX-insensitive Na^+ channels is regulated by a long-term change of the membrane potential. Therefore, it might be assumed that the TTX-insensitive Na^+ channel is suitable for signals which need to be modulated by a relatively slow excitability change. The slow inactivation in TTX-insensitive Na^+ channel may also be related to adaptation, a phenomenon commonly observed in sensation.

Action potential generation and its propagation along the neuronal processes in rat DRG appear to be controlled in a complicated manner depending on the availability of different types of Na^+ channels which are modulated in a time- and voltage-dependent manner by a history of membrane potential change. The somatic sensory system comprises several different perceptual submodalities, each related to different exteroceptive or proprioceptive stimuli. Peripheral sensory neurons process these different types of sensations, and thus, they are themselves a heterogeneous group of cells divided into subpopulations. Kinetic modulation of different types of voltage-gated Na^+ channels may be relevant to the intricate transduction and encoding of different types of sensations.

We thank Prof. Hirosi Kuriyama for his support and advice and Dr. M. Yoshii for helpful discussions. This study was supported by the Japanese Ministry of Education (Scientific Research 02670090).

References

Adams, D.J., Gage, P.W. 1979. Characteristics of sodium and calcium conductance changes produced by membrane depolarization in *Aplysia* neurone. *J. Physiol.* **291**:467–481

Adelman, W.J., Palti, Y. 1969. The effects of external potassium and long duration voltage clamp conditioning on the amplitude of sodium currents in the giant axon of the squid, *Loligo pealei*. *J. Gen. Physiol.* **54**:589–606

Brehm, P., Eckert, R. 1978. Calcium entry leads to inactivation of calcium channel in Paramecium. *Science* **202**:1203–1206

Carmeliet, E. 1987. Slow inactivation of the sodium current in rabbit cardiac Purkinje fibers. *Pfluegers Arch.* **408**:18–26

Chandler, W.K., Hodgkin, A.L., Meves, H. 1965. The effect of changing the internal solution on sodium inactivation and related phenomena in giant axons. *J. Physiol.* **180**:821–836

Chandler, W.K., Meves, H. 1970. Slow changes in membrane permeability and long lasting action potentials in axons perfused with fluoride solutions. *J. Physiol.* **211**:707–728

Chen, Q.X., Stelzer, A., Kay, A.R., Wong, R.K.S. 1990. $GABA_A$ receptor function is regulated by phosphorylation in acutely dissociated guinea-pig hippocampal neurones. *J. Physiol.* **420**:207–221

Fox, J.M. 1976. Ultra-slow inactivation of the ionic currents through the membrane of myelinated nerve. *Biochim. Biophys. Acta* **426**:232–244

Hamill, O.P., Marty, A., Neher, E., Sakmann, B., Sigworth, F.J. 1981. Improved patch-clamp techniques for high-resolution current recording from cells and cell-free membrane patches. *Pfluegers Arch.* **391**:85–100

Hodgkin, A.L., Huxley, A.F. 1952. A quantitative description of membrane current and its application to conduction and excitation in nerve. *J. Physiol.* **117**:500–544

Hotson, J.R., Prince, D.A., Schwartzkroin, P.A. 1979. Anomalous inward rectification in hippocampal neurons. *J. Neurophysiol.* **42**:889–895

Kass, R.S., Scheuer, T. 1982. Slow inactivation of calcium channels in the cardiac Purkinje fiber. *J. Mol. Cell. Cardiol.* **14**:615–618

Kostyuk, P.G., Veselovsky, S., Tsyndrenko, A.Y. 1981. Ionic currents in the somatic membrane of rat dorsal root ganglion neurones. I. Sodium currents. *Neuroscience* **6**:2423–2430

Krishtal, O.A., Pidoplichko, V.I. 1980. A receptor for protons in the nerve cell membrane. *Neuroscience* **5**:2325–2327

McLaughlin, S., Harari, H. 1974. Phospholipid flip-flop and the distribution of surface charges in excitable membranes. *Biophys. J.* **14**:200–208

McNammee, M.G., McConnell, H.M. 1973. Transmembrane potentials and phospholipid flip-flop in excitable membrane vesicles. *Biochemistry* **12**:2951–2958

Narahashi, T. 1964. Restoration of action potential by anodal polarization in lobster giant axons. *J. Cell. Comp. Physiol.* **64**:73–96

Narahashi, T., Tsunoo, A., Yoshii, M. 1987. Characterization of two types of calcium channels in mouse neuroblastoma cells. *J. Physiol.* **383**:231–249

Neumcke, B., Fox, J.M., Drouin, H., Schwarz, W. 1976. Kinetics of the slow variation of peak sodium current in the membrane of myelinated nerve following changes of holding potential or extracellular pH. *Biochim. Biophys. Acta* **426**:245–257

Nilius, B., Kitamura, K., Kuriyama, H. 1992. Properties of inactivation of calcium channel currents in smooth muscle cells of rabbit portal vein. *Am. J. Physiol. (in press)*

Ogata, N., Tatebayashi, H. 1990. Sodium current kinetics in freshly isolated neostriatal neurones of the adult guinea pig. *Pfluegers Arch.* **416**:594–603

Ogata, N., Tatebayashi, H. 1992*a*. Comparison of two types of Na^+ currents with low voltage-activated T-type Ca^{2+} current in newborn rat dorsal root ganglia. *Pfluegers. Arch. (in press)*

Ogata, N., Tatebayashi, H. 1992*b*. Kinetic analysis of two types of Na^+ channels in rat dorsal root ganglia. *J. Physiol. (in press)*

Ogata, N., Tatebayashi, H., 1992*c*. Ontogenic development of the TTX-sensitive and TTX-insensitive Na^+ channels in neurons of the rat dorsal root ganglia. *Dev. Brain Res.* **65**:93–100

Ogata, N., Yoshii, M., Narahashi, T. 1990. Different block of sodium and calcium channels by chlorpromazine in mouse neuroblastoma cells. *J. Physiol.* **420**:165–183

Rudy, B. 1978. Slow inactivation of the sodium conductance in squid giant axons. Pronase resistance. *J. Physiol.* **283**:1–21

Schouten, V.J.A., Morad, M. 1989. Regulation of Ca^{2+} current in frog ventricular myocytes by the holding potential, c-AMP and frequency. *Pfluegers. Arch.* **415**:1–11

Tatebayashi, H., Ogata, N. 1992. Kinetic analysis of the $GABA_B$ mediated inhibition of the high-threshold Ca^{2+} current in cultured rat sensory neurones. *J. Physiol.* **447**:391–407

Received 4 November 1991; revised 5 March 1992